

# Dry demagnetization cryostat for sub-millikelvin helium experiments: refrigeration and thermometry

I. Todoshchenko,<sup>1</sup> J.-P. Kaikkonen,<sup>1</sup> R. Blaauwgeers,<sup>2</sup> P. J. Hakonen,<sup>1</sup> and A. Savin<sup>1</sup>

<sup>1</sup>*O. V. Lounasmaa Laboratory, Aalto University, 00076 AALTO, Finland<sup>a)</sup>*

<sup>2</sup>*BlueFors Cryogenics Ltd, Arinatie 10, 00370 Helsinki, Finland*

We demonstrate successful "dry" refrigeration of quantum fluids down to  $T = 0.16$  mK by using copper nuclear demagnetization stage that is pre-cooled by a pulse-tube-based dilution refrigerator. This type of refrigeration delivers a flexible and simple sub-mK solution to a variety of needs including experiments with superfluid  $^3\text{He}$ . Our central design principle was to eliminate relative vibrations between the high-field magnet and the nuclear refrigeration stage, which resulted in the minimum heat leak of  $Q = 4.4$  nW obtained in field of 35 mT.

For thermometry, we employed a quartz tuning fork immersed into liquid  $^3\text{He}$ . We show that the fork oscillator can be considered as self-calibrating in superfluid  $^3\text{He}$  at the crossover point from hydrodynamic into ballistic quasiparticle regime.

## I. INTRODUCTION

The currently ongoing conversion of sub-Kelvin refrigerators to cryogen-free platforms<sup>1</sup> facilitates new applications (microscopy, imaging, medicine, space applications, security, astronomy, etc) as such systems can be run practically anywhere. Nowadays, dry dilution refrigerators equipped with large superconducting magnets and base temperatures below 10 mK are offered by many suppliers as standard products. Many demanding quantum experiments require a further reduction of temperature.

To meet the above demand, the next challenge is to extend the operation of dry systems to sub-millikelvin temperatures. Nuclear demagnetization cooling<sup>2</sup> combined with a commercially available dry dilution refrigerator as a precooling systems is one of the options to reach the microKelvin regime. Recently, successful operation of such a cryogen-free experimental platform down to 600  $\mu\text{K}$  was demonstrated by Batey *et al.*<sup>3</sup> using a PrNi<sub>5</sub> nuclear stage. However, this temperature is the practical limit for PrNi<sub>5</sub> because of its large intrinsic field, in contrast to copper which enables much lower temperatures. Additionally, copper is more available, easier to handle, and it provides better thermal conductivity when compared with PrNi<sub>5</sub>. As a consequence, most of the modern sub-mK nuclear demagnetization refrigerators employ Cu for the nuclear cooling stage<sup>4-9</sup>. However, Cu stage is more sensitive to external heat loads because of the very demanding precooling conditions to fully polarize the nuclear spins in copper. Furthermore, due to the high electrical conductivity, a good-quality Cu nuclear stage is extremely prone to eddy current heating. All these reasons make nuclear cooling with copper much more difficult to implement on a dry system, but, if successful, also much more rewarding.

Nuclear demagnetization cryostat is quite complicated and laborious machine which includes typically a large

liquid helium bath, a dilution unit, and a large-bore 8-9 Tesla solenoid. The refrigerator requires a large amount of work to construct and to keep operational<sup>2</sup>, and furthermore, its operation needs daily attention. Consequently, for a long time, the investigation of the superfluid  $^3\text{He}$  was a prerogative of big laboratories. This situation will change once a pulse-tube-based dry dilution refrigerator is combined efficiently with a nuclear cooling stage. Such a combination will allow lengthy sub-mK experiments with minimal attention by the operator of the refrigerator.

The aim of this work was to make the first demonstration of superfluid  $^3\text{He}$  refrigeration on a "dry" nuclear demagnetization cryostat all the way down to 0.2 mK. Our central design principle was to eliminate relative vibrations between the high-field magnet and the nuclear refrigeration stage. This principle was found to work quite well and a heat leak of  $Q = 4.4$  nW was obtained at 35 mT. The heat leak was found to scale as  $B^2$  upto  $\sim 100$  mT, which is a clear sign of vibrational heating due to eddy currents. For thermometry, we employed a quartz tuning fork immersed into liquid  $^3\text{He}$ , which indicated 0.16 mK for the lowest temperature. Furthermore, we show that such fork oscillator can be considered as self-calibrating in superfluid  $^3\text{He}$  at the crossover point from hydrodynamic into ballistic quasiparticle regime.

The paper is organized as follows. In the next section the technical details of the cryostat are given. In Section 3 we discuss the thermometry with the tuning fork. The performance of the cryostat is described in Section 4 where we describe the cooling cycle and give the values for the lowest temperatures achieved, the heat leaks in different fields, thermal conductivity of the heat switch, and other details. In Conclusions we summarize the results of our experiments and their analysis.

<sup>a)</sup>Electronic mail: todo@boojum.hut.fi

## II. THE CRYOGEN-FREE DEMAGNETIZATION REFRIGERATOR

Our cryostat is based on the commercially available BF-LD400 dry dilution cryostat from BlueFors Cryogenics<sup>10</sup>. It has a two-stage pulse tube refrigerator with a base temperature of 3 K for the second stage. For condensation of  $^3\text{He}$ - $^4\text{He}$  mixture, the system employs a 2 bar compressor, which can be switched off during continuous circulation. The dilution unit cools down to 7 mK and provides  $550\ \mu\text{W}$  of cooling power at 100 mK. The cryostat has a set of radiation shields thermally anchored at 60 K, 3 K, 0.7 K ( $^3\text{He}$  evaporator) and at the mixing chamber temperature. The cryostat is equipped with a 9 T magnet from American Magnetics which is thermally anchored to the 2nd stage of the pulse tube cooler. In our BF-LD400 the still pumping line and the pulse tube mounting were fitted with the damper systems provided by Bluefors Ltd so that the pulse tube and the turbo pump were mechanically well decoupled from the top flange of the cryostat.

The nuclear stage of the so-called "Helsinki design"<sup>11,12</sup> was made of a single cylindrical copper piece in which a set of slits were machined in order to reduce eddy currents which appear when the enclosed magnetic flux is varying, see Fig. 1. The heat switch which connects the stage and the mixing chamber consists of seven bended aluminium foils ( $50\text{ mm} \times 10\text{ mm} \times 0.5\text{ mm}$  each) diffusion welded to two copper rods, out of which one is bolted to the nuclear stage and the other one to the mixing chamber flange. Before welding, all parts of the heat switch were annealed: copper at  $900\text{ }^\circ\text{C}$  in  $2 \cdot 10^{-3}$  mbar of air for two weeks and aluminium at  $550\text{ }^\circ\text{C}$  in better than  $10^{-5}$  mbar vacuum for 1 hour. A small superconducting solenoid, surrounded by a cylindrical niobium shield, is mounted on the heat switch. A field of 20 mT is employed to drive the aluminium from the superconducting state to the normal state.

The nuclear stage is first pre-cooled in a field of  $B = 8\text{ T}$ ; during this process, the heat switch is in the normal state and thermally connects the nuclear stage to the mixing chamber via electronic thermal conductivity. When the stage approaches the mixing chamber temperature, the heat switch is turned to superconducting state where most of the electrons are bound into Cooper pairs and cannot conduct heat, so that only phonon conductivity is left which is very small at 10 - 20 mK. The magnetic field is then slowly decreased and, in ideal adiabatic conditions, the temperature of copper nuclei is lowered proportionally to  $B^2$ . In reality, some amount of entropy is lost during the demagnetization process due to heat leaks which are to be reduced well below  $1\ \mu\text{W}$  for successful cooling.

Owing to gradients in the polarizing field, eddy currents will be generated in constant field if the nuclear stage vibrates with respect to the magnet. In the case of a "dry" dilution refrigerator, the level of mechanical vi-

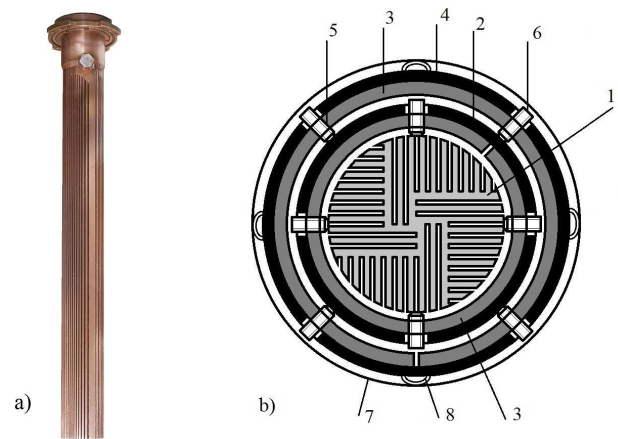


FIG. 1. a) Photograph of the copper nuclear stage with a total length of 438 mm. b) Cross-sectional view of the nuclear stage and radiation shields with spacers: 1 – nuclear stage, 2 – mixing chamber radiation shield, 3 – slotted ring, 4 – 0.7 K radiation shield, 5 – thread, 6 – M4 nylon bolt, 7 – bore of the 9 T magnet, 8 – plastic spring.

brations is significantly higher compared with traditional liquid-He-based refrigerators. Despite the fact that the pulse tube cooler was partly decoupled mechanically from the rest of our cryostat by flexible links, the vibrational heat load to the nuclear stage due to eddy currents was found to be a critical factor for the cooling power of the stage. Initially, there were no spacers between the radiation shields, the magnet, and the nuclear stage, so that the long tail of the nuclear stage vibrated with respect to the magnet, and the eddy currents were producing a heat load of few  $\mu\text{W}$  to the stage in an 8 T field. Addition of spacers, however, reduced the eddy current heating by an order of magnitude.

The employed spacer system is illustrated in Fig. 1b. We have developed an easy way to make spacers between the shields, the magnet and the copper stage for fixing them together without significant changes to the shields. The spacers are made of slotted brass rings with four threaded holes for nylon bolts. The rings are placed between two shields and between the 20-mK shield and the stage. The outer shield has four holes for bolts which tightly press the inner shield, while the ring abuts the outer one, see Fig. 1b. The outer shield has plastic springs to go tightly inside the bore of the magnet. All parts of the stage-shields-magnet assembly are thus strongly mechanically fixed together so that they vibrate as a single piece without significant movements with respect to one another.

The experimental cell for liquid  $^3\text{He}$  is embedded inside the top part of the nuclear stage in a form of a cylinder, and silver sinter with an effective area of about  $20\text{ m}^2$  is baked on the cell walls. In this first experiment, only an oscillating fork was installed inside the cell. Approximately 0.6 mole of  $^3\text{He}$  of 200 ppm  $^4\text{He}$  purity was condensed to the cell. This resulted in a partially filled

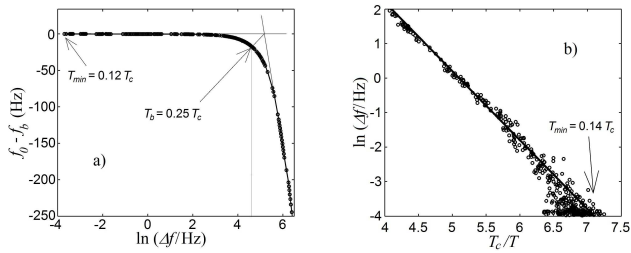


FIG. 2. Preliminary experiment on the self-calibrated fork thermometry in superfluid  $^3\text{He}$  at the melting pressure: a) Crossover from the hydrodynamic to the ballistic regime of oscillating fork at  $\ln(\Delta f/\text{Hz}) \approx 4.5$ . The lowest temperature is  $0.12 T_c$ , according to Eq. (1). b) Logarithm of the width of the resonance as a function of inverse reduced temperature measured using melting curve thermometer. The fit shows slope -2, in agreement with Eq. (1) where  $\Delta = 2.0 T_c$ <sup>15</sup>. The lowest temperature is  $0.14 T_c$ .

chamber with a free liquid-vapor interface.

### III. THERMOMETRY

The thermometry of helium sample in the sub-millikelvin range is quite a difficult task. The thermal boundary resistance, Kapitza resistance, between (dielectric) helium and the copper refrigerant increases as  $1/T^3$ . This means that even tiny heat leak to helium sample will saturate temperature of helium at the level determined by the heat leak and surface area of thermal contact, while the copper is much colder. Because of this thermal decoupling of helium from the environment it is absolutely necessary to measure the temperature of liquid  $^3\text{He}$  directly. There are three practical ways to determine liquid  $^3\text{He}$  temperature by measuring a) nuclear magnetic susceptibility of helium with NMR b) melting pressure with a sensitive *in situ* transducer, and c) density of quasiparticles with a mechanical oscillator. Unfortunately, the temperature dependence of susceptibility of superfluid  $^3\text{He}$  saturates below  $0.5 T_c$ , and thus NMR thermometry is not useful at the lowest temperatures. Moreover, the sensitivity of the melting curve thermometer also rapidly decreases at low temperatures. In contrast to these two thermometers, the sensitivity of a mechanical oscillator rapidly increases with lowering temperature<sup>13</sup>. In the ballistic regime below  $\sim 0.3 T_c$ , where the mean free path of quasiparticles becomes larger than the size of the oscillator, the fluid-induced damping decreases exponentially,  $\Delta f \propto \exp(-\Delta/T)$  where  $\Delta f$  is the width of the resonance of the oscillator and  $\Delta$  is the superfluid energy gap. This behavior has been predicted theoretically by Guénault *et al.*<sup>14</sup> and demonstrated experimentally by Todoshchenko *et al.*<sup>15</sup> using a vibrating wire in combination with melting curve thermometry.

Mechanical oscillator thermometer is, however, a secondary thermometer and as such it needs to be calibrated against some other thermometer. Even in the ballistic

regime, it needs calibration at least at one temperature in order to scale the width of the resonance with respect to it. Fortunately, the oscillator can be used to calibrate itself. The idea is to use the central frequency of the resonance as an independent single-point (“fixed point”) thermometer. In the hydrodynamic regime there is an additional mass attached effectively to the oscillator due to the viscous motion of quasiparticle excitations around it. Upon cooling, the mean free path of quasiparticles increases rapidly, and less and less quasiparticles around the oscillator feel its motion and the effective mass of the oscillator decreases. The central frequency of the resonance is inversely proportional to the square root of the effective mass, and it saturates once the mean free path becomes longer than the size of the oscillator. Hence, the point of the crossover from the hydrodynamic regime into the ballistic regime is manifested by a saturation of the dependence of central frequency  $f_0$  as a function of the width of the resonance  $\Delta f$  (see Fig. 2a).

The onset of the ballistic regime is quite exactly determined because the dependence of the mean free path on temperature is very steep<sup>16</sup>. The calibration procedure is thus to measure the width  $\Delta f_b$  at which central frequency  $f_0$  saturates and attribute this width to certain temperature  $T_b$  depending on the size of the oscillator. Then the temperatures below  $T_b$  can be calculated according to an exponential scaling law

$$\frac{\Delta f}{\Delta f_b} = \exp\left[\frac{\Delta}{T_b} - \frac{\Delta}{T}\right], \quad (1)$$

where  $\Delta f_b$  refers to the width at the onset temperature  $T_b$ . The superfluid energy gap  $\Delta$  is temperature-independent below  $0.5 T_c$ <sup>17</sup> and varies with pressure from  $1.8 T_c$  at zero bar to  $2.0 T_c$  at the melting pressure<sup>15</sup>. This simple exponential law together with the evident single-point calibration at the onset of the ballistic regime makes the mechanical oscillator as a very sensitive “primary” thermometer.

The self-calibration property has proven to work reliably at the melting pressure according to independent simultaneous temperature measurements using melting curve thermometry; this experiment was done on a regular nuclear demagnetization cryostat for  $^3\text{He}$ <sup>18</sup>. The melting curve thermometer was a capacitive Straty-Adams strain pressure gauge<sup>19</sup> with  $\sim 5 \mu\text{bar}$  accuracy. The resonator in these cross-check experiments was a commercially available quartz tuning fork with 0.6 mm wide tines, which had exactly the same dimensions as in the present work. According to the calculations by Ono *et al.*<sup>16</sup>, the onset of the ballistic regime for this size is at  $T_b = 0.25 T_c$ . The crossover from hydrodynamic to ballistic behavior is viewed best by plotting the central frequency  $f_0$  versus logarithm of the resonance width  $\Delta f$  as shown in Fig. 2a. The onset of the ballistic regime, which we determine as the maximum of the second derivative of the function  $f_0 = f_0(\ln(\Delta f/\text{Hz}))$ , occurs at  $\ln(\Delta f_b/\text{Hz}) = 4.5$ . The lowest measured width

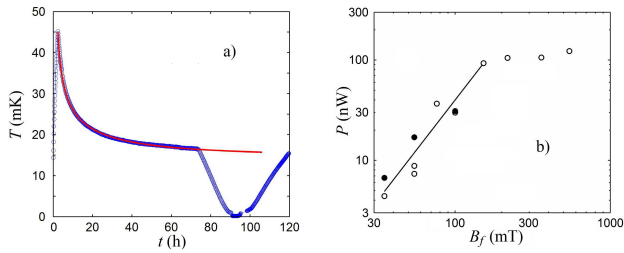


FIG. 3. a) Temperature of liquid  $^3\text{He}$  inside the nuclear stage. Magnetization towards 8 T started at time  $t = 0$  and was completed at  $t = 2.4$  h. At  $t = 74$  h the heat switch was turned off and the magnetic field sweep from 8 T down to 35 mT was started. Superfluid transition was reached at time  $t = 90.5$  h in a field of 250 mT. The curve is the fit of the precool process using Eq. (3) with  $1.4 \mu\Omega$  for the resistance of the heat switch and with a heat leak of  $P = 250$  nW, see the text for details. b) The heat leak to the nuclear stage as a function of the final demagnetization field  $B_f$ . Open symbols – empty cell, closed symbols – cell is partially filled with liquid  $^3\text{He}$ . The straight line corresponds to the expected, eddy-current-induced  $B^2$  dependence at low fields.

corresponds to  $\ln(\Delta f_{min}/\text{Hz}) = -3.9$  which, according to Eq. (1), yields  $T_{min} = \Delta/(4.5 + 3.9 + \Delta/T_b)$ . By substituting  $\Delta = 2.0 T_c$  for the superfluid energy gap at high pressure and  $T_b = 0.25 T_c$  for the onset we find  $T_{min} = 0.12 T_c$ . The apparent arbitrariness in the determination of the onset location, *i. e.*  $T_b$ , does not affect significantly the accuracy of the method due to sharpness of the crossover. Indeed, if we take 4 or 5 instead of 4.5 for the  $\ln(\Delta f_b/\text{Hz})$ , it will result in a very small change of the minimum temperature, ranging from  $0.125 T_c$  to  $0.118 T_c$ . An independent measurement of  $\ln(\Delta f/\text{Hz})$  vs  $T$  using melting curve thermometry, Fig. 2b, yields  $0.14 T_c$  for the minimum temperature. The agreement with the result  $T_{min} = 0.12 T_c$  based on the self-calibration method is quite good if one considers the relatively large heat capacity of solid  $^3\text{He}$  which keeps the solid-liquid interface at a temperature slightly higher than that of the liquid.

In addition to the fork resonances, the temperature of the demagnetization stage was also recorded by a noise thermometer manufactured by Physical-Technical Institute (Physikalisch-Technische Bundesanstalt) in Berlin using the electronics from Magnicon Ltd.<sup>20</sup> The sensitive element of the noise thermometer is a copper block, the thermal noise currents of which are recorded by a SQUID that is picking up the magnetic flux induced by the noise currents. The noise thermometer was mechanically attached to the nuclear demagnetization stage with 5 mm long threaded stud at the end of the copper block. We found that this system worked well on the dry dilution refrigerator despite the magnetic noise from the pulse tube heat exchangers<sup>21</sup>. It was found that temperatures down to 0.4 mK could be recorded on the nuclear stage using the noise thermometer. The saturation of the noise thermometer at temperatures below 0.4 mK is due to the

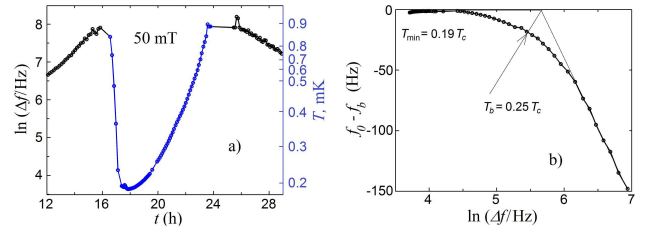


FIG. 4. a) Logarithm of the width of the resonance in liquid  $^3\text{He}$  at zero pressure. Demagnetization was started at time  $t = 0$  and was finished at  $t = 17.5$  h. On cooling,  $T_c$  was passed at  $t \simeq 16.5$  h after which the width  $\Delta f$  rapidly decreased by two orders of magnitude. At  $t = 18$  h, warm-up began and  $T_c$  was passed again at  $t = 24$  h. The temperature axis on the right is obtained from the ballistic exponent below 0.3 mK and using the width data by Eltsov *et al.*<sup>23</sup> at  $0.3 \text{ mK} < T < 0.9 \text{ mK}$  scaled to the size of our fork. Temperature axis refers only to superfluid state from 16.5 to 24 hours. b) Crossover from the hydrodynamic to the ballistic regime for the motion of the oscillating fork (from left to right). The saturation of the central frequency  $f_0$  occurs at  $\ln(\Delta f/\text{Hz}) \simeq 4.5$ . The lowest temperature is  $0.19 T_c$  according to the self-calibration method.

heat leak of  $\sim 200$  pW from the SQUID bias.

#### IV. PERFORMANCE OF THE REFRIGERATOR

Fig. 3a depicts a full operation cycle of our demagnetization cryostat. The cooldown starts by running the dilution unit at a high circulation rate of  $\sim 800 \mu\text{mol/s}$ , which cools the nuclear stage below 20 mK through the heat switch which is kept in the conducting (normal) state by its small magnet. Prior to the demagnetization cycles, the experimental chamber inside the nuclear stage, was filled by 0.6 moles of  $^3\text{He}$  at low pressure to immerse the tuning fork fully inside liquid. In the normal fluid state above  $T_c = 0.93 \text{ mK}$ <sup>22</sup>, the width of the fork resonance  $\Delta f$  is inversely proportional to temperature<sup>23</sup>. The calibration of the fork for measurements in the normal state of  $^3\text{He}$  was made at  $T_c$  during the demagnetization process.

In Fig. 3a, the field in the main magnet was ramped up from 0 to 8 T in 2.5 hours. Precooling of the nuclear stage at 8 T was continued for about three days; this time is mostly determined by the thermal conductance of the present heat switch and the heat capacity of the nuclear stage. Our copper nuclear stage has effectively 3.5 kg in the high field region, which means that its nuclear heat capacity is  $C \simeq 1.7 \cdot 10^{-4} B^2/T^2 \text{ JK/T}^2 = A/T^{22}$ , where field-dependent constant  $A$  equals 0.012 JK in 8 T field. The heat balance can be written as

$$P dt - \frac{A}{T^2} dT - \frac{T^2 - T_0^2}{\gamma} dt = 0 \quad (2)$$

where  $P$  is the heat leak to the nuclear stage,  $\gamma$  is the thermal resistance of the heat switch, and  $T_0 = 14$  mK is the ultimate temperature of the dilution unit under 8 T conditions. After integration, we find

$$t - t_1 = \frac{\gamma A}{\Theta^2} \left[ \frac{1}{T_1} - \frac{1}{T} + \frac{1}{2\Theta} \ln \frac{(T_1 - \Theta)(T + \Theta)}{(T_1 + \Theta)(T - \Theta)} \right], \quad (3)$$

where  $\Theta = \sqrt{P\gamma + T_0^2}$  is a characteristic temperature of the demagnetization refrigerator, which accounts for the temperature of the dilution unit, for the heat leak to the nuclear stage, and for the quality of the heat switch.

Eq. (3) fits well the experimentally measured temperature during precooling as seen in Fig. 3a. From the fit we find the heat leak to the nuclear stage  $P = 250$  nW and the thermal resistance of the switch  $\gamma = 120$  K<sup>2</sup>/W. If the temperature difference  $\delta T = T - T_0$  over the heat switch is relatively small, then the heat flux through the switch can be written as  $\dot{Q} = (2T/\gamma)\delta T$ . It is more convenient to express the thermal resistance in units of electrical (temperature-independent) resistance  $R = \gamma L/2 = 1.4$   $\mu\Omega$ , where  $L = 2.4 \cdot 10^{-8}$  W $\Omega$ /K<sup>2</sup> is the Lorenz number. After the precool, at time  $t = 75$  h, the heat switch is turned to superconducting state and the field is slowly swept down to 50 mT.

We applied fork thermometry with self-calibration (see Sect. 3) to measure the lowest temperature achieved in superfluid <sup>3</sup>He on our refrigerator. Similar fork as in the experiment at the melting pressure was employed meaning that the onset temperature  $T_b$  for the ballistic regime must again be  $0.25 T_c$ . Fig. 4a displays the logarithm of the fork resonance width  $\Delta f$  as a function of time. Near  $T_c$ ,  $\Delta f$  becomes of the order of the central frequency  $f_0$  and the resonance is basically lost until the liquid enters the superfluid state at  $t = 16.5$  h. With growing superfluid fraction, the width decreases rapidly over two orders of magnitude and, finally at  $\Delta f \sim 300$  Hz, the fork is in the regime where Eq. (1) becomes applicable. The liquid still cools a bit further down to  $\Delta f = 40$  Hz which corresponds to  $T = 0.19 T_c = 0.17$  mK according to Eq. (1). While warming,  $T_c$  is passed again at  $t = 24.0$  h. From the warmup rate we can calculate the heat leak to the nuclear stage to be about 25 nW in a final demagnetization field  $B_f$  of 50 mT. During the next demagnetization cycle to a field of 35 mT, we have measured even a smaller fork resonance width of 15 Hz corresponding to  $T = 0.16$  mK. Note that the sensitivity of the fork thermometer is so high at lowest temperatures that the decrease of the width by 2.5 times means only 5% difference in temperature.

During these demagnetization experiments, we also followed the nuclear stage temperature by noise thermometry. Unfortunately, the reading from the noise thermometer was limited to  $T > 0.40$  mK due to overheating of the copper block by the SQUID bias current. At  $T > 1$  mK, the noise thermometer worked well and was instrumental in our heat leak measurements at high  $T$ .

At low values of the final demagnetization fields  $B_f$ , the heat leak to the nuclear stage was found to depend linearly on  $B_f^2$  as illustrated in Fig. 3b. This means that the warmup rate does not actually depend on the field as both the heat capacity of the stage and the heat leak are proportional to  $B_f^2$  (provided that  $B_f \gg B_{int} = 0.3$  mT). At fields higher than 50-100 mT, however, the field dependence of the heat leak becomes gradually slower and the warmup rate decreases correspondingly. Indeed, instead of a typical 7 hours below  $T_c$ , we stayed in our best cool downs at  $B_f = 100$  mT in the superfluid state for 14 hours. This time span, which can be extended to  $\sim 20 - 25$  hours by further demagnetization from 100 mT, can be regarded as fully adequate for basic experiments in superfluid <sup>3</sup>He. The minimum heat leak to the nuclear stage of 4.4 nW was measured in 35 mT field with empty cell. Typically, the heat leaks with the cell filled with <sup>3</sup>He were somewhat higher compared to empty cell because of the viscous heating of <sup>3</sup>He due to vibrations.

## V. CONCLUSIONS

We have demonstrated cooling of <sup>3</sup>He well below the superfluid transition temperature  $T = 0.93$  mK at saturated vapor pressure using a helium-free "dry" demagnetization refrigerator. Our work is the first to cool helium-3 down to 0.16 mK on a LHe-bath-free refrigerator, and thus we open an opportunity for deep sub-mK investigations on a commercially available pulse tube refrigerator straightforwardly equipped with a copper adiabatic nuclear demagnetization stage. In our work, we have introduced a new simple method to measure the temperature of superfluid <sup>3</sup>He via the properties of mechanical fork oscillators without the need for other thermometers for calibration. The method has proven to work accurately at the melting pressure when compared against an independent melting curve thermometer.

## ACKNOWLEDGEMENTS

We are grateful to Juha Tuoriniemi, Matti Manninen, and Juho Rysti who took part in the thermometry experiments at the melting pressure. The work was supported by the Academy of Finland (contracts no. 135908 and 250280, LTQ CoE and FIRI2010) and the EU 7th Framework Programme (FP7/20072013, grant Microkelvin). This research project made use of the Aalto University Cryohall infrastructure.

## REFERENCES

- <sup>1</sup>K. Uhlig, *Cryogenics* **42**, 73 (2002);
- <sup>2</sup>K. Anders and O. V. Lounasmaa, *Progress in Low Temperature Physics* **VIII**, 221 (1982).

- <sup>3</sup>G. Batey, A. Casey, M. N. Cuthbert, A. J. Matthews, J. Saunders, and A. Shibahara, *New J. Phys.* **15**, 113034 (2013).
- <sup>4</sup>P. M. Berglund, G. J. Ehnholm, R. G. Gylling, O. V. Lounasmaa, and R. P. Sovik, *Cryogenics* **12**, 297 (1972).
- <sup>5</sup>D. I. Bradley, A. M. Guénault, V. Keith, I. E. Miller, S. J. Mussett, G. R. Pickett, and W. P. Pratt, *J. Low Temp. Phys.* **57**, 359 (1984).
- <sup>6</sup>M. T. Huiki, T. A. Jurkkiö, J. M. Kyynäräinen, O. V. Lounasmaa, and A. S. Oja, *J. Low Temp. Phys.* **62**, 433 (1986).
- <sup>7</sup>A. S. Borovik-Romanov, Yu. M. Bunkov, V. V. Dmitriev, and Yu. M. Muharsky, *Japan. J. Appl. Phys.* **26**, 1719 (1987).
- <sup>8</sup>K. Gloos, P. Smeibidl, C. Kennedy, A. Singsaas, P. Sekowski, R. M. Mueller, F. Pobell, *J. Low Temp. Phys.* **73**, 101 (1988).
- <sup>9</sup>J. Xu, J. S. Xia, M-F. Xu, T. Lang, P. I. Moyland, W. Ni, E. D. Adams, G. G. Ihas, M. W. Meisel, N. S. Sullivan, and Y. Takano, *J. Low Temp. Phys.* **89**, 719 (1992).
- <sup>10</sup>BlueFors Cryogenics Oy Ltd, Arinatie 10, 00370 Helsinki, Finland. www.bluefors.com.
- <sup>11</sup>J. P. Pekola, J. T. Simola, and K. K. Nummila, *10th International Conference on Cryogenic Engineering (ICEC10)*, eds. P. Berglund and M. Krusius (Guilford, UK, 1984) p. 259.
- <sup>12</sup>R. H. Salmelin, J. M. Kyynäräinen, M. P. Berglund, and J. P. Pekola, *J. Low Temp. Phys.* **76**, 83 (1989).
- <sup>13</sup>A. M. Guénault, V. Keith, C. J. Kennedy, I. E. Miller, and G. R. Pickett, *Nature* **302**, 695 (1983).
- <sup>14</sup>A. M. Guénault, V. Keith, C. J. Kennedy, S. J. Mussett, and G. R. Pickett, *J. Low Temp. Phys.* **62**, 511 (1986).
- <sup>15</sup>I. A. Todoshchenko, H. Alles, A. Babkin, A. Ya. Parshin, and V. Tsepelin, *J. Low Temp. Phys.* **126**, 1449 (2002).
- <sup>16</sup>Y. A. Ono, J. Hara, K. Nagai, *J. Low Temp. Phys.* **48**, 167 (1982).
- <sup>17</sup>B. Mühlischlegel, *Zeit. für Physik* **155**, 313 (1959).
- <sup>18</sup>M. S. Manninen, J.-P. Kaikkonen, V. Peri, J. Rysti, I. Todoshchenko, J. Tuoriniemi, *J. Low Temp. Phys.* **175**, 56 (2014).
- <sup>19</sup>G. S. Straty and E. D. Adams, *Rev. Sci. Instr.* **40**, 1393 (1969).
- <sup>20</sup>J. Beyer, M. Schmidt, J. Engert, S. AliValiollahi and H. J. Barthelmess, *Supercond. Sci. Technol.* **26**, 065010 (2013)
- <sup>21</sup>M. J. Eshraghi, I. Sasada, J. M. Kim, and Y. H. Lee *Cryogenics* **49**, 334 (2009).
- <sup>22</sup>D. S. Greywall, *Phys. Rev. B* **33**, 7520 (1986).
- <sup>23</sup>R. Blaauwgeers, M. Blazkova, M. Človečko, V. B. Eltsov, R. de Graaf, J. Hosio, M. Krusius, D. Schmoranzler, W. Schoepe, L. Skrbek, P. Skyba, R. E. Solntsev, and D. E. Zmeev, *J. Low Temp. Phys.* **146**, 537 (2007).